

Simulation of three-dimensional Ising spin glass model using three replicas: study of Binder cumulants

This article has been downloaded from IOPscience. Please scroll down to see the full text article.

1996 J. Phys. A: Math. Gen. 29 4337

(<http://iopscience.iop.org/0305-4470/29/15/009>)

View [the table of contents for this issue](#), or go to the [journal homepage](#) for more

Download details:

IP Address: 171.66.16.70

The article was downloaded on 02/06/2010 at 03:56

Please note that [terms and conditions apply](#).

Simulation of three-dimensional Ising spin glass model using three replicas: study of Binder cumulants

David Iñiguez^{†‡§}, Giorgio Parisi^{‡||} and Juan J Ruiz-Lorenzo^{‡¶}

[†] Departamento de Física Teórica, Universidad de Zaragoza, P San Francisco s/n 50009 Zaragoza, Spain

[‡] Dipartimento di Fisica and Infn, Università di Roma, La Sapienza, P A Moro 2, 00185 Roma, Italy

Received 15 March 1996

Abstract. We have carried out numerical simulations of the three-dimensional Ising spin glass model with first neighbour Gaussian couplings using three replicas for each sample of couplings. We have paid special attention to the measure of two types of Binder cumulant that can be constructed from the three possible overlaps between the replicas. We obtain new information about the possible phase transition and perform an initial analysis of the ultrametricity issue.

1. Introduction

The problem of the existence or not of a phase transition in three-dimensional spin glasses is still a subject of controversy [1]. In the last year a lot of work has appeared with the purpose of clarifying the existence or not of the phase transition, and in the first case, characterizing the critical exponents [2–4]. Moreover recent numerical work has shown that the low temperature phase is as predicted by mean field [5]. Also recent analytical work by Guerra [6] has clarified the meaning of some formulae found in the framework of the mean field theory.

The most relevant observable in the study of these systems is the overlap between replicas, i.e. the order parameter of the system. Up to now, all simulations have been carried out with only two replicas for each sample of couplings. The principal novelty we introduce in this paper is the use of three replicas.

A way to study a possible phase transition is to use the Binder cumulant. This quantity clearly marks the change to a Gaussian situation from the non-Gaussian one. At present this approach has not been very successful for spin glasses because at low temperatures the results turn out to be inconclusive. One needs a lot of statistics and large lattices to obtain the small deviation between curves corresponding to different sizes.

In this paper we study two types of Binder cumulant constructed from the three different overlaps we can measure between the three replicas. The objective is to obtain a clearer signal than in the case of two replica cumulant. From one cumulant, which shows a signal very similar to the two replica ones, we have estimated the critical temperature and the exponent ν on the paramagnetic side, obtaining a good agreement with the previous

§ E-mail address: david@sol.unizar.es

|| E-mail address: parisi@roma1.infn.it

¶ E-mail address: ruiz@chimera.roma1.infn.it

quoted values [2]. The other cumulant presents new and interesting features and supplies us a method of studying the possible ultrametricity of the spin glass phase as well as a determination of the critical temperature.

2. Model, simulation and observables

The model we have studied is the three-dimensional Ising spin glass with nearest-neighbour couplings distributed Gaussianly around zero. The Hamiltonian is

$$\mathcal{H} = - \sum_{\langle i, j \rangle} J_{ij} \sigma_i \sigma_j. \quad (1)$$

As usual $\langle i, j \rangle$ denotes nearest-neighbour pairs. The lattice sizes we simulated are $L = 4, 6, 8, 10$. We have used the simulated tempering method [7, 8]. The range of temperatures studied has been [0.7, 1.3] (for $L = 4$ we have also made a run in the range [0.3, 1.3]) in steps of 0.05. We have simulated 4096 different samples of couplings for $L = 4, 6$ and 2048 samples for $L = 8, 10$, with three replicas for each sample[†].

The number of sweeps depends slightly on the lattice size, but it is typically one million for measuring, after the order of half a million iterations to estimate the free energy. The calculations have been carried out on a *tower* of APE100 [9] with a real performance, for this problem, of five Gigaflops for a total time of three weeks. The errors, sample to sample, have been computed with the jack-knife method.

As a check of the thermalization procedure we have monitored the symmetry of the distribution of the overlaps (i.e. $P(q) = P(-q)$). We have also checked the two following relations [6]:

$$\overline{\langle q^2 \rangle^2} = \frac{2}{3} \overline{\langle q^2 \rangle}^2 + \frac{1}{3} \overline{\langle q^4 \rangle} \quad (2)$$

$$\overline{\langle q^2 q'^2 \rangle} = \frac{1}{2} \overline{\langle q^2 \rangle}^2 + \frac{1}{2} \overline{\langle q^4 \rangle}. \quad (3)$$

As usual, we denote thermal averages by $\langle (\cdot) \rangle$ and disorder averages by $\overline{(\cdot)}$. The first formula (2) was pointed out in a previous numerical analysis [5], and has been rigorously demonstrated, along with (3), by Guerra [6]. Both relations are well satisfied by our data for every value of L and T . Their validity has been proved in the infinite volume limit, however, it is possible that the deviations are small also for not too large volumes, as those of the present paper.

We have focused our attention on the following Binder cumulants constructed from the three overlaps measured for each sample of couplings:

$$B_{qqq} \equiv \frac{\overline{\langle |q_{12} q_{13} q_{23}| \rangle}}{\overline{\langle q^2 \rangle}^{3/2}} \quad B'_{qqq} \equiv \frac{\overline{\langle q_{12} q_{13} q_{23} \rangle}}{\overline{\langle q^2 \rangle}^{3/2}} \quad (4)$$

and

$$B_{q-q} \equiv \frac{\overline{\langle (|q_{12}| - |q_{13}|)^2 \rangle}}{\overline{\langle q_{23}^2 \rangle}} \quad B'_{q-q} \equiv \frac{\overline{\langle (q_{12} - q_{13} \text{sign}(q_{23}))^2 \rangle}}{\overline{\langle q_{23}^2 \rangle}} \quad (5)$$

where q_{23} is the largest one (in absolute value). These definitions must follow the finite size scaling relation

$$B_{\#} = f_{\#}(L^{1/\nu}(T - T_c)) \quad (6)$$

[†] Let σ , τ and μ be the three replicas that we will simulate in parallel with the same disorder. Hence, we can define three different overlaps that we will denote $\{q_{12}, q_{23}, q_{13}\}$ or $\{q, q', q''\}$ indiscriminately in the rest of the paper.

where we have used the symbol # to denote either cumulant. In the following sections we will study, in detail, these observables.

3. B_{qqq} and B'_{qqq}

In figure 1 the values obtained from the simulations for B_{qqq} are shown (lower curves). We observe that at high temperatures the values for the different lattice sizes are widely separated (the larger L the smaller B_{qqq}). However, below $T \approx 1.1$ the curves intermingle. In order to distinguish them clearly it would be necessary to considerably reduce the errors. The observable B'_{qqq} presents a similar behaviour. In fact, the product $q_{12}q_{13}q_{23}$ is generally positive (because it is favoured combinatorially even if one has three completely independent configurations).

In the same figure, we show the values we would expect if the three overlaps satisfied ultrametricity (upper curves). We have calculated these curves in the following way. The probability distribution of the overlaps for each temperature and lattice size, $P(q)$, is obtained directly from the simulations. From it we extract the function $x(q)$ defined as

$$x(q) = \int_0^q dq' P(q') \quad (7)$$

and then we obtain the inverse $q(x)$, which is shown in figure 2 for different temperatures at $L = 10$. Supposing ultrametricity† [10]

$$P_3(q, q', q'') = \frac{1}{2} P(q)x(q)\delta(q - q')\delta(q - q'') + \frac{1}{2}(P(q)P(q')\theta(q' - q'')\delta(q'' - q) + \text{two permutations}) \quad (8)$$

the cumulant will take the value

$$B_{qqq} = \frac{1}{(\int_0^1 dx q^2(x))^{3/2}} \left(\frac{3}{2} \int_0^1 dx q^2(x) \int_x^1 dy q(y) + \frac{1}{2} \int_0^1 dx x q^3(x) \right). \quad (9)$$

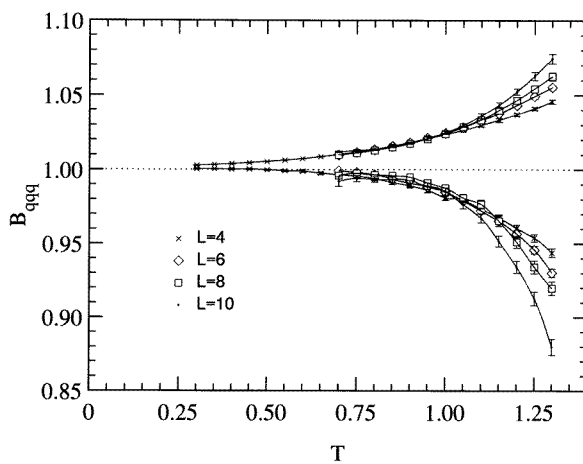


Figure 1. B_{qqq} against T : numerical data (lower curves) and supposing ultrametricity (as explained in the text) (upper curves).

† In the appendix we will show that if ultrametricity, convexity and positivity hold then the functional form of $P_3(q, q', q'')$ must be that of mean field for a generic $P(q)$.

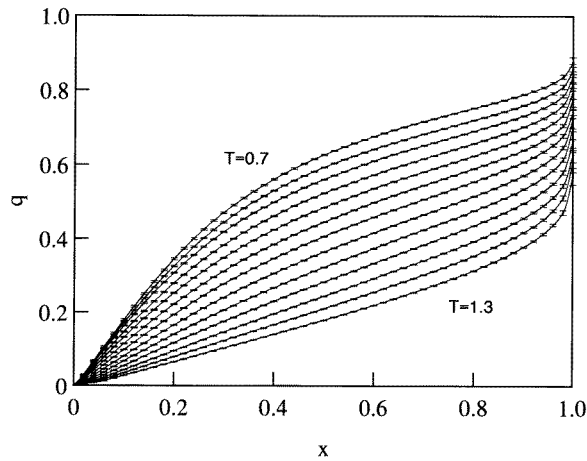


Figure 2. $q(x)$ for 13 different temperatures.

We can observe that the curves extracted directly from the simulations approach those obtained supposing ultrametricity when the temperature decreases. This is in agreement with the fact that ultrametricity could be expected at low temperatures. However, it is not a demonstration because practically any reasonable type of relation (including independence) between the q 's would produce curves approaching the value 1 when the temperature goes to zero. On the other hand, the curves from the simulations are under the value 1 (the points for $L = 4$, $T = 0.3$ – 0.4 are over 1 but contain this value inside their error bars) while the lines' bases on ultrametricity always remain greater than 1. These results do not rule out the possibility that the overlaps are as independent as possible for any temperature (even when the three replicas are totally independent, the probability of the three overlaps has a constraint given by a simple combinatorial problem); when decreasing the temperature the behaviour of the $P(q)$ favours the B_{qqq} approaching 1.

The equation (9) can also be used to see what would be obtained if we assume for $q(x)$ a shape that could be expected in the thermodynamic limit, that is to say

$$q(x) = \begin{cases} q_0 \left(\frac{x}{m}\right)^r & 0 < x < m \\ q_0 & \text{otherwise.} \end{cases} \quad (10)$$

We would obtain

$$B_{qqq} = \frac{1}{\left(1 - \frac{2r}{2r+1}m\right)^{3/2}} \left[1 - \frac{3r}{2r+1}m + \frac{3}{4} \left(1 - \frac{2r^2 + 7r + 2}{6r^2 + 7r + 2}\right)m^2 \right]. \quad (11)$$

In figure 2 we observe that the function $q(x)$ obtained from the simulations is rather similar to the supposed here with $m = 1$ and r descending from approximately 1 for high temperature towards 0 as the temperature diminishes. As a test, we can compare qualitatively the curves shown in figure 1 in the case of ultrametricity with a function of this type, and it is seen that in fact the behaviour is similar.

We have estimated the value of the exponent ν by fitting the derivative of B_{qqq} in the high temperature region as

$$f(g, L) \equiv \left. \frac{dB_{qqq}}{dT} \right|_{T_0: B_{qqq}(T_0)=g} = \alpha L^{1/\nu}. \quad (12)$$

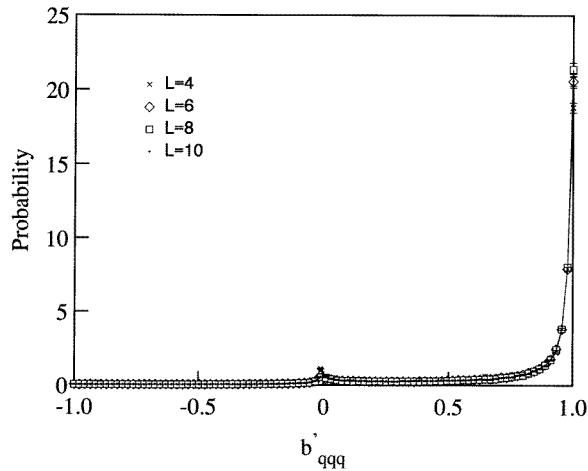


Figure 3. Probability to have a b'_{qqq} value for the four different sizes and $T = 0.8$.

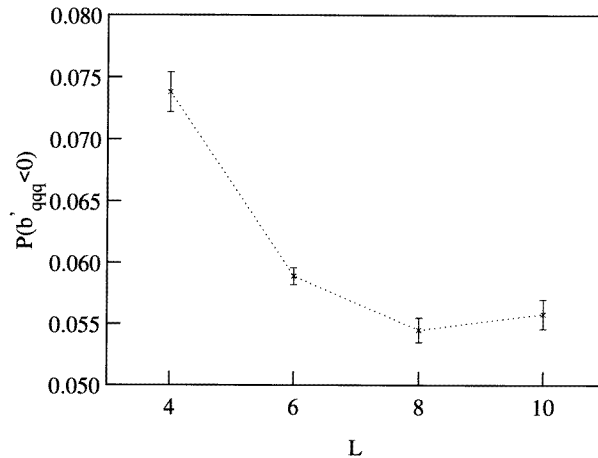


Figure 4. Scaling, as a function of size, of the area of the negative part ($b'_{qqq} < 0$) in figure 3.

We have used polynomials of different orders to fit $B_{qqq}(T)$ and calculated the derivatives at several values of B_{qqq} . Let us remark that these derivatives are taken at different values of T but at fixed B_{qqq} . All the results obtained for ν , for different values of g near the critical one $g_c \equiv B_{qqq}(T_c)$, are compatible within the errors, which turn out to be large. Finally, we give an estimation of $\nu = 1.5(3)$, which is in good agreement with the value $\nu = 1.7(3)$ reported in [2] for the $\pm J$ spin glass.

As we have remarked above, the product $q_{12}q_{13}q_{23}$ is mainly positive, but not always. In figure 3 we show the probability distribution of

$$b'_{qqq} \equiv \frac{q_{12}q_{13}q_{23}}{(\frac{1}{3}(q_{12}^2 + q_{13}^2 + q_{23}^2))^{3/2}} \quad (13)$$

for the different L values at $T = 0.8$. Figure 4 attempts to show how the area of the negative part behaves with L , but it is not clear if it will go to zero with increasing L or not. If mean field holds the negative area must go to zero.

4. B_{q-q} and B'_{q-q}

As can be seen in figure 5, B_{q-q} has a much clearer signal than B_{qqq} . We observe a crossing of the curves for different L in the region $T \approx 1$. At low temperatures the values for $L = 10$ mask an inversion of the curves (i.e. the larger L the smaller B_{q-q} while the high temperature order is the other way round) which is very clear for $L = 4, 6, 8$, as shown in the expanded figure 5(b). From the crossing of the curves for the larger lattices we can estimate a critical temperature of approximately $T_c = 1.02(5)$. B'_{q-q} also presents similar behaviour.

These observables, B_{q-q} and B'_{q-q} , would be zero if ultrametricity were exactly verified. In any case, we expect violations of ultrametricity due to the finite size of our lattice as happens in the SK model [11]. The same considerations as in the preceding section can be made regarding the approach of the B_{q-q} curves to zero when the temperature decreases.

A trial of estimating ν as above gives results that move systematically with the value B_{q-q} fixed and then it has been discarded.

We have made a study of the probability distribution of

$$b \equiv \frac{(|q_{12}| - |q_{13}|)^2}{q_{23}^2} \quad (14)$$

(where q_{23} is the biggest one) calculated at every single iteration, at temperature $T = 0.8$.

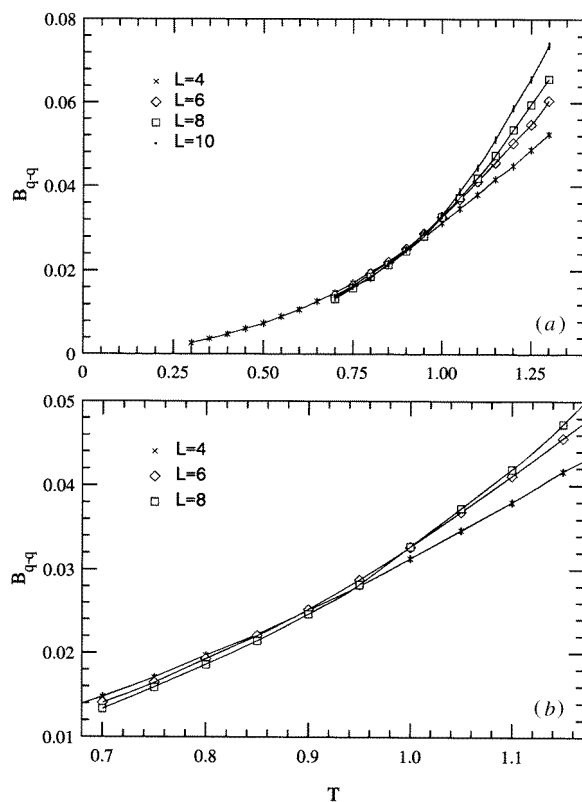


Figure 5. (a) B_{q-q} versus T for the four different sizes. In (b) we plot only $L = 4, 6, 8$ and $T \in [0.7, 1.3]$.

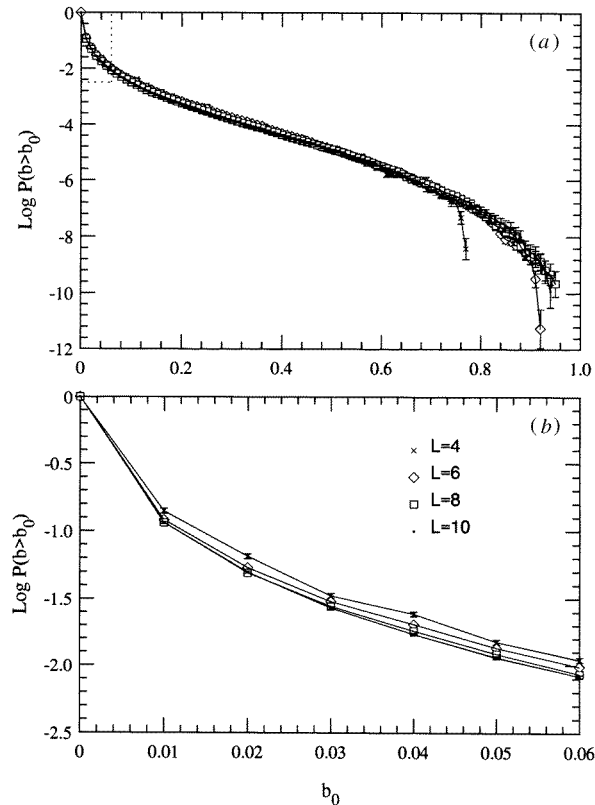


Figure 6. Plot of the accumulated probability for all the points (a) and only for a window near the origin (b).

In figure 6 we show the logarithm of the probability of having a value of b larger than a certain b_0 versus b_0 . Figure 7 has the same variable on the vertical axis but the logarithm of b_0 on the horizontal one. The curves for the different values of L are hardly distinguishable. Expanding the image in the region of small b_0 (figures 6(b) and 7(b)), we see that the upper curves are those of smaller L corresponding to bigger B_{q-q} , but the lowering with L is slow and it is difficult to guess any asymptotic behaviour. Selecting, for instance, a value of $b_0 = 0.05$ and observing how this probability decreases with L we find approximately a power law with a small exponent of 0.13(2). In the region of large b_0 , the upper curves correspond to larger L (in order to maintain the total probability normalized). For all the values of L , we observe a first region, for small b_0 , where the decrease of probability can be approximated by a power behaviour of the form $b_0^{-\alpha}$ with $\alpha = 0.71(2)$. There is a central *plateau* where it decreases exponentially as $e^{-\alpha b_0}$ with α ranging from 5.8(1) for $L = 4$ to 5.3(1) for $L = 10$, while it goes to zero faster when b_0 approaches the geometrical limit of 1.

The observable

$$b' \equiv \frac{(q_{12} - q_{13} \text{sign}(q_{23}))^2}{q_{23}^2} \quad (15)$$

shows a similar behaviour.

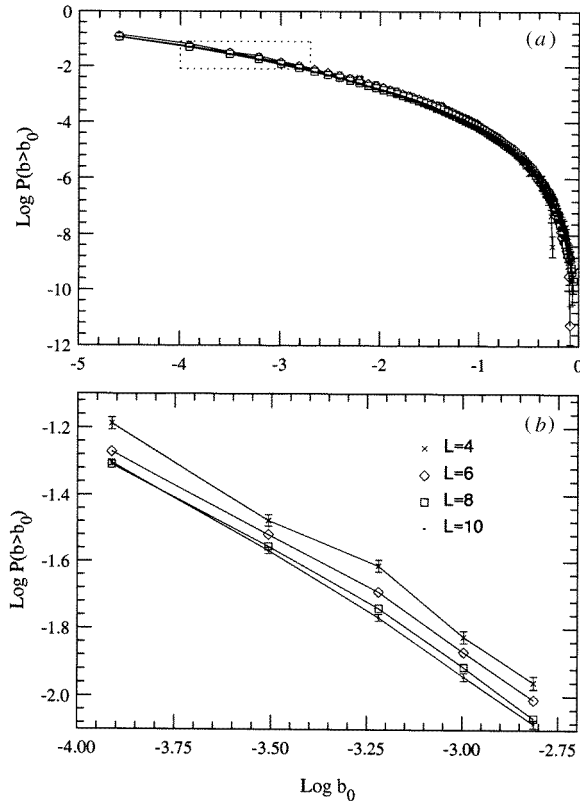


Figure 7. The same as figure 6 but in a double log scale.

5. Conclusions

We have reported in this paper a study of the three-dimensional Ising spin glass model using three replicas. In particular we have studied different versions of the Binder cumulant with three replicas. We have estimated both the transition points as well as the critical exponent ν being in good agreement with previous reported values [2].

Using one of the Binder cumulants we have begun a preliminary study of ultrametricity. We have found that the b probability distribution goes to zero following a power law. These results are not conclusive (the exponent is small) and we will need to simulate large lattices using new thermalization methods (for instance parallel tempering [3]) in order to distinguish between lack of ultrametricity and possible violations due to finite size effects.

Acknowledgments

We acknowledge useful discussions with E Marinari and D Lancaster. D Iñiguez thanks MEC and CAI. J J Ruiz-Lorenzo is supported by an EC HMC(ERBFMBICT950429) grant.

Appendix

In this appendix we will show that if ultrametricity holds as well as convexity and positivity then the three-replica probability must be the mean field one.

The most general formula, using the invariance of the Hamiltonian under the exchange of replicas, for the probability of three replicas assuming ultrametricity is:

$$P_3(q, q', q'') = A(q)\delta(q - q')\delta(q - q'') + B(q, q')\theta(q - q')\delta(q' - q'') \\ + B(q', q'')\theta(q' - q'')\delta(q'' - q) + B(q'', q)\theta(q'' - q)\delta(q - q') \quad (A1)$$

with $A(q)$ and $B(q, q')$ satisfying normalization condition and $B(x, y) = B(y, x)$. Integrating q'' we obtain the probability to have two replicas:

$$P_2(q, q') = \left[A(q) + \int_q^\infty dq'' B(q', q'') \right] \delta(q - q') + B(q, q') \quad (A2)$$

and finally the probability of one replica ($P(q)$ that we will denote, in this appendix, as $P_1(q)$) is

$$P_1(q) = A(q) + \int_q^\infty dq' B(q, q') + \int_{-\infty}^\infty dq' B(q, q'). \quad (A3)$$

Now we impose the relation (demonstrated by Guerra using only positivity and convexity)

$$\overline{\langle q^2 q'^2 \rangle} \equiv \int_{-\infty}^\infty dq dq' P_2(q, q') q^2 q'^2 = \frac{1}{2} \overline{\langle q^2 \rangle}^2 + \frac{1}{2} \overline{\langle q^4 \rangle} \quad (A4)$$

where

$$\overline{\langle q^n \rangle} = \int_{-\infty}^\infty dq P_1(q) q^n.$$

We finally obtain the following equations:

$$A(q) = \int_{-\infty}^q dq' B(q, q') \quad (A5)$$

$$B(q, q') = 2 \left(\int_{-\infty}^\infty dq'' B(q, q'') \right) \left(\int_{-\infty}^\infty dq'' B(q', q'') \right). \quad (A6)$$

Joining equations (A3) and (A5)

$$P_1(q) = 2 \int_{-\infty}^\infty dq' B(q, q') \quad (A7)$$

and then we recover the mean field formulae, i.e.

$$A(q) = \frac{1}{2} x(q) P_1(q) \quad (A8)$$

$$B(q, q') = \frac{1}{2} P_1(q) P_1(q') \quad (A9)$$

with a free $P_1(q)$. Obviously this development does not imply any particular functional form for $P_1(q)$.

References

- [1] Rieger H 1995 *Annual Reviews of Computational Physics II* (Singapore: World Scientific) p 295
- [2] Kawashima N and Young P *Report cond-mat/9510009*
- [3] Hukushima K and Nemoto K *Report cond-mat/9512035*
- [4] Marinari E, Parisi G and Ruiz-Lorenzo J J Work in progress
- [5] Marinari E, Parisi G, Ruiz-Lorenzo J J and Ritort F 1996 *Phys. Rev. Lett.* **76** 843
- [6] Guerra F *Int. J. Mod. Phys. B* in press
- [7] Marinari E and Parisi G 1992 *Europhys. Lett.* **19** 451
- [8] Marinari E, Fernández L A and Ruiz-Lorenzo J J 1995 *J. Physique I* **5** 1247
- [9] Battista C *et al* 1993 *Int. J. High-Speed Comput.* **5** 637
- [10] Mezard M, Parisi G and Virasoro M A 1987 *Spin Glass Theory and Beyond* (Singapore: World Scientific)
- [11] Bath R N and Young P 1986 *J. Magn. Magn. Mater.* **54-57** 191